Special Issue Article

Journal of Intelligent Material Systems and Structures

Journal of Intelligent Material Systems and Structures
2016, Vol. 27(7) 872–879

DOI: 10.1177/1045389X15596624
jim.sagepub.com
SAGE

Synergy between magnetorheological fluids and aluminum foams: Prospective alternative for seismic damping

M Aguilera Portillo[1], P Santa Ana Lozada[1], IA Figueroa[2], MA Suárez[2], AV Delgado[3] and GR Iglesias[3]

Abstract

This article presents the experimental study of a preliminary investigation of a seismic damper device aimed at improving the behavior of structures when subjected to earthquakes. The damper is the result of a binomial material formed by an aluminum foam with pores of 1 mm diameter wetted by a magnetorheological fluid. The objective of this work is to explore the synergy between the two components on a magnetorheological test and to evaluate the effect of the Al foam pores in the structure buildup of the fluid. The analysis is completed with a compressive test carried out on the magnetorheological fluid–filled foam in the presence of a magnetic field. This kind of test demonstrates that the deformation of the foam for very small loads is limited by the hardening of the fluid because of its magnetorheological response. The results of this research suggest that there is a mutual benefit between the components of the device, presumably leading to an enhanced dissipation of vibration energy.

Keywords

Magnetorheological fluid, dissipation of energy, seismic damper, metal foam, magnetorheological analysis

Introduction

A magnetorheological fluid (MRF) is a kind of intelligent material typically in the form of a complex fluid with a high concentration of magnetizable microparticles dispersed in a nonmagnetic fluid (Bossis et al., 2002; Carlson and Jolly, 2000; De Vicente et al., 2011; Lopez-Lopez et al., 2006; Velte et al., 2011). Other formulations, including mixed micro- and nanoparticles, or nonmagnetic holes in a ferrofluid (Rodriguez-Arco et al., 2014), are possible, but not so generally used in applications. Its name comes, in any case, from the fact that the application of an often homogeneous magnetic field produces an increase in the apparent viscosity of the suspension, and a modification of the rheological behavior from Newtonian to viscoelastic, with yield stress or elastic modulus up to 100 kPa (Phulé et al., 1999). These changes occur in a few milliseconds and are removed reversibly when the magnetic field is switched off (Baranwal and Deshmukh, 2008; Chacón Hernando, 2009). This rheological ability to control the structure is due to well-defined particle chain structures formed by the alignment of the magnetic moments of the particles in the field direction (Furst and Gast, 2000).

The strength of the magnetorheological (MR) effect is directly related to the amount, size distribution, shape, density, saturation magnetization, and coercivity of the magnetic particles in the suspension, as well as to the intensity of the magnetic field applied. The dispersed phase can be either a ferri- or ferromagnetic material, usually consisting of soft magnetic particles, including iron, magnetite, or other ferrites (Carlson and Jolly, 2000).

Since their discovery in the 1940s, the application of MR suspensions has forged its way into several branches of technological development including industrial areas such as aerospace (Park et al., 2010), biomedical prostheses, drug vehicle design (López and Gallardo, 2006), and mechanical engineering. In the

[1]Faculty of Architecture, National Autonomous University of Mexico, Mexico D.F., Mexico
[2]Institute of Materials Research, National Autonomous University of Mexico, Mexico D.F., Mexico
[3]Department of Applied Physics, School of Science, University of Granada, Granada, Spain

Corresponding author:
GR Iglesias, Department of Applied Physics, School of Sciences, University of Granada, 18071 Granada, Spain.
Email: iglesias@ugr.es

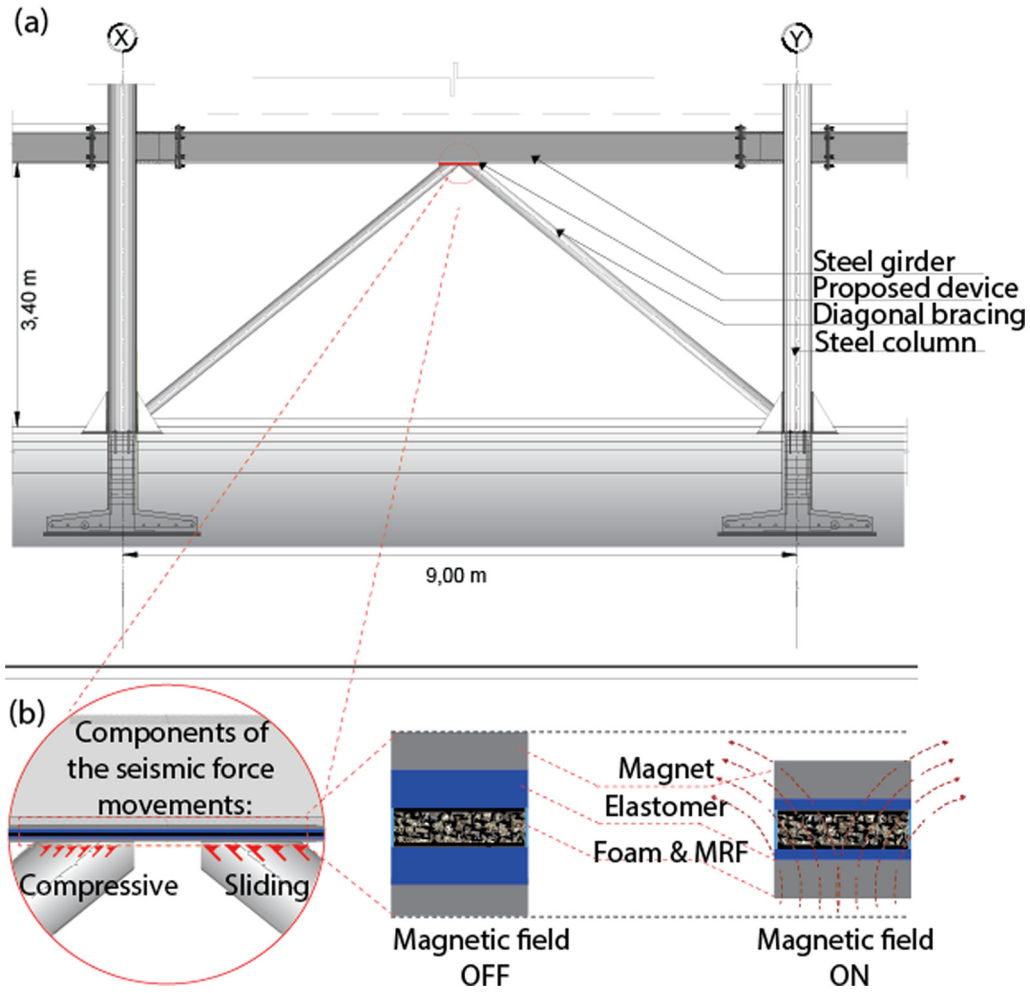

Figure 1. (a) Theoretical location of the energy-dissipating devices in the architecture structural system and (b) details of the operation: configurations in field-off and field-on conditions.

latter, brakes, shock absorbers, vibration controllers, dampers, and seismic insulators (Bhatti, 2012; Eem et al., 2013; Gordaninejar et al., 2010; Rossa et al., 2014a, 2014b) have been devised.

In the particular field of architecture, the importance of the creation of light and resistant materials that provide damping is a continuous need. Inspired by natural cellular materials, either metallic or polymeric foams have been designed which are capable of dissipating strain energy when subjected to mechanical vibration under cyclic deformation (Banhart, 2001; Fusheng et al., 1999). Recently, there have been proposals of MR dampers aiming at these applications, based on the incorporation of metallic foams as support for the MRF (Carlson, 1999; Liu, 2010; Liu et al., 2010; Yao et al., 2013). The MRF in this case would be confined in the foam without the need of expensive, degradable seals, and as a result, these devices may become a good option for low-cost absorber production.

Based on the above explanation, in this work, the design and mechanical analysis of a seismic impact-absorbing device are proposed, using the MR effect in a composite system formed by an aluminum foam filled with an MRF. The final aim of the project would be to build a panel for steel structures from 1- to 6-story frames so as to improve protection during an earthquake. The first step is the study of the synergy between the MRF and an aluminum foam with highly interconnected pores. This will be carried out at the laboratory scale, starting from the evaluation of the MR response of the composite structure. The research methodology used was based on the *Technology Readiness Level* as instrument for the creation and incorporation of products in the market. Ideally, the MR foam could be implemented in a structure as illustrated in Figure 1. A common method to increase the stiffness of structural frames is the addition of diagonal braces. In order to design earthquake-resisting buildings, engineers propose the incorporation of energy-dissipating devices, at the joint with the steel gilder (Figure 1(a)), such as added damping and stiffness (ADAS) or triangular added damping and stiffness (TADAS) metallic dampers (Alehashem et al., 2008). These kinds of devices absorb and dissipate energy

during earthquakes, due to the movement of the upper end of the passive device, relative to the lower end, which causes yielding of the plates composing it. This location has great concentration of displacement, which causes shear stress in the building materials. As shown in Figure 1(b), the MRF–foam device is also proposed in a passive configuration: a pair of magnets will confine the MRF in the foam, and when the seismic wave goes in the structure, the magnet approaches the foam inducing the MR effect, thus hampering the movement from the diagonal bracing to the steel gilder and reducing the amount of seismic energy to be dissipated in the upper story frames of the structure.

Experimental

Aluminum foam elaboration: metal infiltration method

The infiltration method consists of the casting and injection of a molten metal in a preform, and it can be applied to a large variety of metals (Figueroa Vargas et al., 2012). In our case, the foams were made from industrial aluminum (Alfa Aesar, Mexico), with 99.9% purity and density of 2.7 g/cm^3. This selection was made because of its diamagnetic behavior, low cost, abundance on earth's surface, easy recyclability, and high stiffness in combination with a comparatively low density (Gutiérrez-Vázquez and Oñoro, 2008).

The procedure was performed in the following steps:

1. For the pellet preparation, a mixture containing 22% (by weight) water, 68% NaCl, and 10% flour was prepared until a consistent dough was obtained, capable of spreading spontaneously. A 1-cm-thick layer was produced, dried at ambient conditions for 2 days, and ground to the desired size (approximately 1 mm) in a mortar.
2. The pellets (total 415 g) were poured in a cylindrical, stainless steel 316, crucible 27 cm in height and 10 cm in outer diameter. The crucible was heated for 1 h in a preheated furnace at 200 °C. After this extensive drying, the preform was calcined at 350 °C for 30 min.
3. In total, 700–1000 g of aluminum was placed on top of the preform and a vacuum of 5.5×10^{-2} Torr was produced under an Ar protective atmosphere which was maintained while the crucible was placed in the furnace and preheated at 600–750 °C, depending on the required interconnectivity.
4. The final cylindrical foams were 5 mm in height and 2.54 cm in diameter. Two kinds of preparations were selected for this study, as detailed in Table 1. Figure 2 shows the different steps in the preparation.

Table 1. Al foam samples selected for the MR damper study.

Sample	Dough mass (g)	Density (g/cm^3)	Porosity (%)
1	2.52	0.9968	63
2	2.12	0.8415	69

MR: magnetorheological.

MRF preparation

HQ carbonyl iron powder from BASF (Germany) was used as solid phase. It consists of spherical particles with a median particle size of $d_{50} = 2.3\,\mu m$ (particle diameters range from 0.5 to 3 μm) and an iron content of 97% (density = 7.5 g/cm^3). The base carrier fluid was mineral oil (Sigma–Aldrich, USA), and it was used for all the suspensions; its viscosity at 25 °C is 0.028 ± 0.001 Pa s. The solid concentrations used were 25%, 30%, 35%, 40%, and 45% v/v. Additives for stabilizing the particles were incorporated as described in Durán et al. (2008).

The MR characterization of the fluids tested was carried out in an MCR300 Rheometer from Physica–Anton Paar (Austria), provided with an MR device (Physica MRD). The magnetic circuit is designed so that the magnetic flux lines are normal to the parallel disks. A parallel plate (20 mm in diameter) configuration was used, with a 7-mm gap. This is rather large but was necessary because of the thickness of the Al foam disks supporting the fluids. In the manufacturer's design, a yoke covering the upper plate allows for a quite homogeneous magnetic field through the sample volume. With the modification necessary for our tests, the yoke was placed 5 mm above its normal working position. Because in such configuration the homogeneity of the field might be compromised, we measured its normal component using a GM08 gaussmeter from Hirst Magnetic Instruments Ltd (UK), with a 100-μT resolution. In our case, the maximum variation of the field along the diameter was less than 5%, and vertically along the axis, it was 10% at most. Thus, although the homogeneity is partially sacrificed, the results are still meaningful in the context of this investigation. In order to keep the fluid in a fixed position, we used a thin plastic container surrounding the foam and fluid film. The bottom plate of the MRF is the aluminum foam piece, with very rough surface. The top plate is serrated to avoid wall slip.

A controlled rate mode was used, with shear rates ranging between 1 and 50 s^{-1} and a test duration of 120 s. Samples were pre-sheared at 30 s^{-1} for 60 s and subsequently left to equilibrate under the action of the field during a further 60 s, before the application of the shear ramp. All experiments were conducted at 25 °C ± 1 °C.

Figure 2. Illustration of the different steps of the Al foam preparation: (a) untreated pellets, (b) dried and calcined pellets, (c) controlled-atmosphere crucible, (d) resulting foam, and (e) the same after cleaning with water and ultrasounds.

Preparation of the magnetic foams

Four different foam–MRF preparations were studied, named A, B, C, and D, as described in Table 2. Sample A is the pure MRF, used for the sake of comparison. The maximum MR response is expected in this case. Samples C and D constitute the mixed systems, and they differ in the porosity of the metal foam (63% and 69%, respectively). Finally, we designate by B the sample consisting of MRF deposited on a solid aluminum piece. It can be considered as a contrast sample to ensure that any effects observed in C and D are not just the result of effectively reducing the cell gap, rather the result of the foam–MRF synergistic behavior.

Mechanical compressive analysis

In order to test the composites in somewhat realistic conditions, that is, when working under compression and not just under shear, we carried out a compressive analysis by placing the magnetic foams in the home-made test cell depicted in Figure 3. A compressive stress was applied on top of the mobile cover using a SPECAC 25.011 (UK) manual press, capable of applying up to 15 T force or 1.43 MPa pressure. Both the spindle in the compressive machine and the cover of the device (shown in Figure 3) had a diameter of 2.54 cm. The magnetic field was applied by passing a current of up to 2.5 A along a coil surrounding the container (1270 turns, copper wire 0.7 mm in diameter); the highest magnetic field in the samples was 150 mT (in air). The MRF used for this evaluation was the one containing 45% v/v concentration of solids.

Results and discussion

MR analysis of the suspensions and magnetic foams

Figure 4 shows typical rheograms for the pure MRF with 45% Fe, using two gaps, the ideal one (1 mm plate distance) and the one to be used when the foam is in the rheometer cell (7 mm). Note that the behaviors are similar in both cases, and the obvious difference that the maximum field attainable is smaller in the second case is the only observation worth to consider. A straightforward consequence of this fact is the reduction of the maximum shear stress for the same

Table 2. Samples description and exponent n of the power-law fitting of yield stress as a function of field strength with 45% v/v concentration ($\tau_y = mB^n$) for each of them.

System	A	B	C	D
		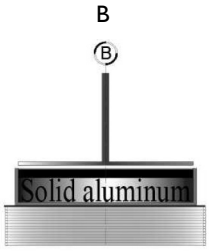	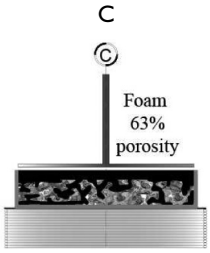	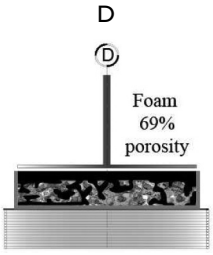
% of MRF	100	68.2	65.2	49.9
Volume contained (mL)	5	3.41	3.26	2.47
Exponent, n	2.3 ± 0.1	1.6 ± 0.1	1.5 ± 0.1	0.9 ± 0.1

MRF: magnetorheological fluid.

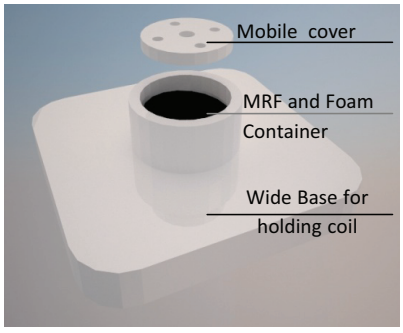

Figure 3. Cell used for the compression tests.

rate. Let us also point out that for the two experimental conditions the samples show yield stress increasing with the field strength. The yield stress was evaluated by fitting the rheograms to the Bingham equation (the so-called dynamic yield stress), and the results are presented in Figure 5, in the form of yield stress τ_y versus magnetic field strength. Note that the field dependence of the yield stress is parabolic in the pure MRF, but the power exponent n of the fittings $\tau_y = mB^n$ (Table 2) is smaller for the foam–MRF systems: the presence of the metallic foam appears to hinder the formation of particle chains by dipolar interactions, due to the confinement of the MR fluid.

Normal force determinations were also carried out in all cases. The conclusions drawn on the shear stress results are largely confirmed in that kind of analysis, as Figure 6 demonstrates for a typical situation ($50\,s^{-1}$ shear rate, 45% volume fraction of iron in the MRF). The best MR response corresponds to sample C (comparable or even better than the pure fluid). The decreased porosity of sample B and its absence in sample D reduce the synergy between the metal and fluid components.

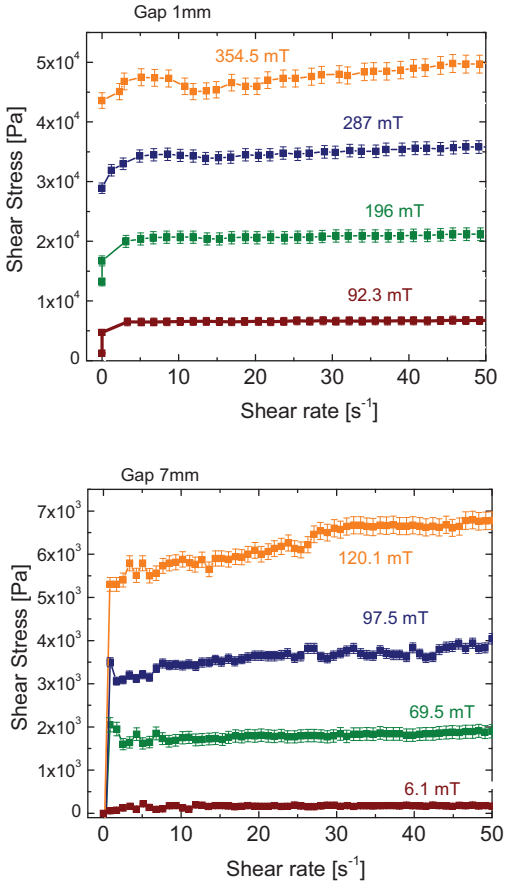

Figure 4. Shear stress as a function of shear rate for the 45% MRF and cell gaps of 1 mm (top) and 7 mm (bottom).

Mechanical compressive analysis

The strain of the aluminum foam normally displays three stages, and it is expected that the MRF will be able to extend the first one, namely, elastic strain. The

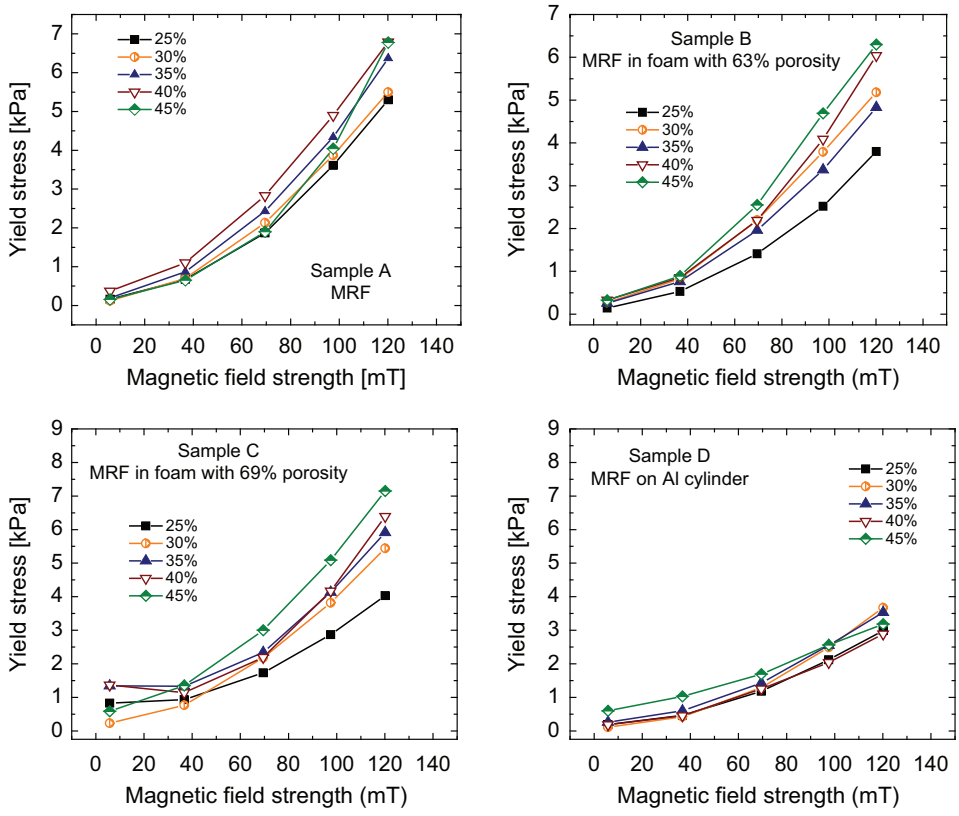

Figure 5. Yield stress as a function of magnetic field strength for the MR fluid and 7 mm gap (sample type and iron concentrations are indicated in the figures).

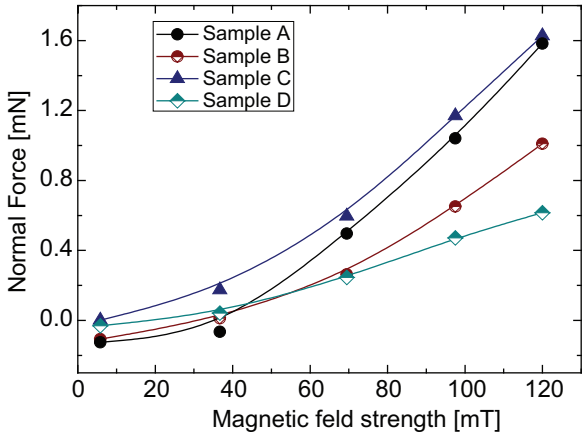

Figure 6. Normal force during the MR determinations detailed in Figure 5, for samples A (MRF), B (MRF + 63% foam), C (MRF + 69% foam), and D (MRF + Al cylinder). In all cases, the shear rate was 50 s^{-1}, and the concentration of iron particles was 45%.

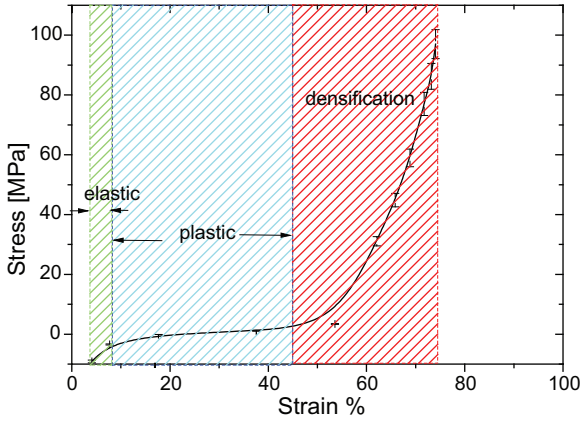

Figure 7. Compression test for an Al foam on the compression machine. Test tube: ∅ 25.4 mm; height, 20 mm; spindle speed, 0.5 mm/min; and test load, 8 ton.

second and third ones, that is, plastic deformation and densification (Figure 7), are not in the interest of this work. The whole test is illustrated by the pictures in Figure 8.

The results of tests performed on type C (foam porosity 69% and 45% v/v MRF) MRF–foam composite with and without magnetic field are represented in Figure 8. It can be observed that the magnetic field increases the resistance of the MRF–foam device to undergo deformation for given stress, a very significant result of this proof-of-concept investigation. This behavior can be justified based on the fact that the MRF–foam needs to be covered or enclosed so that the liquid cannot escape, when the magnetic field is off. However,

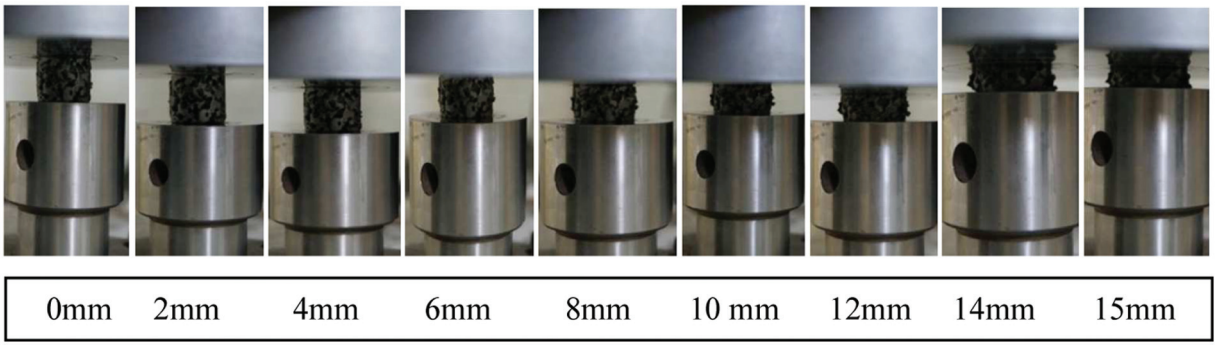

Figure 8. Photographs taken during the compression test of the aluminum foam.

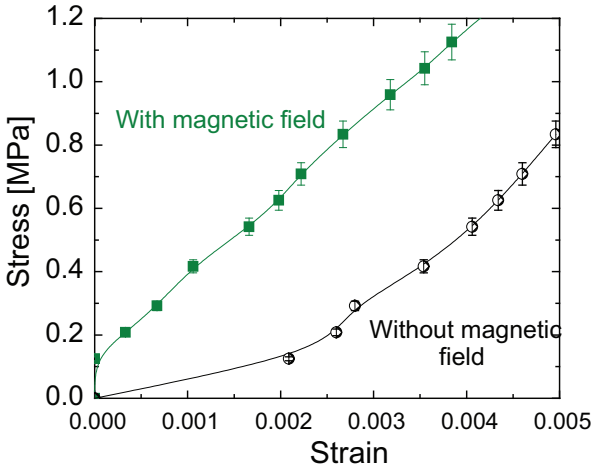

Figure 9. Compression test results, for sample C and 45% v/v iron in the MRF.

if the magnetic field is applied, the state of aggregation of the MRF will be semisolid and the MR effect will try to prevent the densification of the foam, by forming the Fe chains oriented with the magnetic field. However, we have the compressive force that will try to break those chains leading to internal friction between both materials. The resulting balance, as Figure 9 shows, indicates the possibility of control of the mechanical behavior of the foam–MRF composite through magnetic field strength variations.

Conclusion

As a proof of concept of an MR damper, a composite system based on the combination of a metal (aluminum) foam and an MRF has been prepared and tested. MR determinations confirm that the system behaves from the rheological point of view in a similar way as the pure magnetic fluid, except for a minor decrease in the apparent dynamical Bingham yield stress, but with the advantage of a much lower amount of fluid, necessary for filling the pores of the foam. The MR behavior is different from that found by the simple juxtaposition of an Al block and a fluid layer on top of it. This shows that the sought synergy takes place. This is even more clear in compression tests: the deformation for a given pressure is considerably smaller in the foam–MRF system if the field is applied, precisely the final aim of this kind of devices. Although a very extensive investigation is still necessary, we believe that the idea is worth to be explored since the two expected roles of these systems (magnetic field response and capacity to dissipate mechanical energy) appear to be present in the simple composites described.

Declaration of Conflicting Interests

The authors declared no potential conflicts of interest with respect to the research, authorship, and/or publication of this article.

Funding

The author(s) disclosed receipt of the following financial support for the research, authorship, and/or publication of this article: Financial support was provided by projects PE2012-FQM694 (Junta de Andalucía, Spain), FIS2013-47666-C3-1-R, SENER-CONACYT "151496" (UNAM Mexico), and CONACYT National Quality Graduate Program. Institute of Materials Research, National Autonomous University of Mexico (Mexico) also provided support.

References

Alehashem SMS, Keyhani A and Pourmohammad H (2008) Behavior and performance of structures equipped with ADAS & TADAS dampers (a comparison with conventional structures). In: *The 14th world conference on earthquake engineering*, Beijing, China, 12–17 October.

Banhart J (2001) Manufacture, characterisation and application of cellular metals and metal foams. *Progress in Materials Science* 46: 559–632.

Baranwal D and Deshmukh TS (2008) MR-Fluid technology and its application—a review. *International Journal of Emerging Technology and Advanced Engineering* 2: 563–569.

Bhatti AQ (2012) Performance of viscoelastic dampers (VED) under various temperatures and application of

magnetorheological dampers (MRD) for seismic control of structures. *Mechanics of Time-Dependent Materials* 17: 275–284.

Bossis G, Volkova O, Lacis S, et al. (2002) Magnetorheology: fluids, structures and rheology. *Lecture Notes in Physics* 594: 202–230.

Carlson JD (1999) Low-Cost MR fluid sponge devices. *Journal of Intelligent Material Systems and Structures* 10: 589–594.

Carlson JD and Jolly MR (2000) MR fluid, foam and elastomer devices. *Mechatronics* 10: 555–569.

Chacón Hernando V (2009) *Designing a Suspension for a Motor Vehicle Based on Magneto-Rheological Dampers*. Madrid: Polytechnic School of the University Carlos III of Madrid.

De Vicente J, Klingenberg DJ and Hidalgo-Alvarez R (2011) Magnetorheological fluids: a review. *Soft Matter* 7: 3701–3710.

Durán JDG, González Caballero F, Delgado AV, et al. (2008) Magnetorheological fluid. Patent P200602735-EPO 7119395.7

Eem SH, Jung HJ and Koo JH (2013) Seismic performance evaluation of an MR elastomer-based smart base isolation system using real-time hybrid simulation. *Smart Materials and Structures* 22: 055003.

Figueroa Vargas IA, GÁ Lara Rodriguez, Novelo Peralta O, et al. (2012) *Manual for Production of Metal Foams by Infiltration: Introduction and Description of the Production Process by Infiltration*. Mexico D.F., Mexico: Institute of Materials Research, National Autonomous University of Mexico.

Furst EM and Gast AP (2000) Micromechanics of magnetorheological suspensions. *Physical Review E: Statistical Physics, Plasmas, Fluids, and Related Interdisciplinary Topics* 61: 6732–6739.

Fusheng H, Zhengang Z, Changsong L, et al. (1999) Damping behavior of foamed aluminum. *Metallurgical and Materials Transactions A* 30: 771–776.

Gordaninejar F, Wang X, Hitchcock G, et al. (2010) Modular high-force seismic magneto-rheological fluid damper. *Journal of Structural Engineering* 136: 135–143.

Gutiérrez-Vázquez JA and Oñoro J (2008) Review: aluminum foams—manufacture, properties and applications. *Journal of Metallurgy* 44: 457–476.

Liu XH (2010) Shear performance of novel disk-type porous foam metal magneto-rheological (MR) fluid actuator. *Optoelectronics and Advanced Materials* 4: 1346–1349.

Liu XH, Wong PL, Wang W, et al. (2010) Feasibility study on the storage of magnetorheological fluid using metal foams. *Journal of Intelligent Material Systems and Structures* 21: 1193–1200.

López J and Gallardo V (2006) *Magneto-rheological fluids in aqueous medium*. Doctorial Thesis, University of Granada, Granada.

Lopez-Lopez MT, Kuzhir P, Lacis S, et al. (2006) Magnetorheology for suspensions of solid particles dispersed in ferrofluids. *Journal of Physics: Condensed Matter* 18: S2803–S2813.

Park BJ, Fang FF and Choi HJ (2010) Magnetorheology: materials and application. *Soft Matter* 6: 5246–5253.

Phulé PP, Mihalcin MP and Genc S (1999) The role of dispersed-phase remnant magnetization on the redispersibility of magnetorheological fluids. *Journal of Materials Research* 14: 3037–3041.

Rodriguez-Arco L, Lopez-Lopez MT, Zubarev AY, et al. (2014) Inverse magnetorheological fluids. *Soft Matter* 10: 6256–6265.

Rossa C, Jaegy A, Lozada J, et al. (2014a) Design considerations for magnetorheological brakes. *IEEE: ASME Transactions on Mechatronics* 19: 1669–1680.

Rossa C, Jaegy A, Micaelli A, et al. (2014b) Development of a multilayered wide-ranged torque magnetorheological brake. *Smart Materials and Structures* 23: 025028.

Velte D, Jiménez I, Murillo N, et al. (2011) *Foresight Report New Smart Materials*. Spanish Foundation for Science and Technology (FECYT), Madrid.

Yao XY, Lui XH, Yu M, et al. (2013) Dynamic response time of a metal foam magneto-rheological damper. *Smart Materials and Structures* 22: 025026.